Constraints from neutrino masses and muon (g-2) in the bilinear R-parity violating supersymmetric model

R. S. Hundi[1,*]

[1] *Department of Theoretical Physics,*
Indian Association for the Cultivation of Science,
2A & 2B Raja S.C. Mullick Road, Kolkata - 700 032, India.

Abstract

Bilinear R-parity violating supersymmetric model is a viable model which can explain the smallness of neutrino masses and the mixing pattern in the lepton sector. In this model, there is a common set of parameters which determine the neutralino and chargino masses, also determine the neutrino masses and the anomalous magnetic moment of muon, $(g-2)_\mu$. From the experimental data on neutrino masses and mixing angles, and also from the fact that the experimentally measured value of $(g-2)_\mu$ differs from the corresponding standard model value by 3σ, we have analyzed some constraints on these model parameters. Constraints on these model parameters are obtained for some values of supersymmetry breaking soft parameters. These constraints can set upper and lower bounds on the chargino masses of this model.

* tprsh@iacs.res.in

I. INTRODUCTION

Since the discovery of neutrinos, their mass estimation has provoked much excitement among particle phenomenologists. The deficit in the neutrino flux from solar [1] and atmospheric [2] neutrinos have confirmed that at least two neutrinos should have non-zero masses. The recent global fitting to the various neutrino experimental data has given the following mass-squared differences and mixing angle values at 1σ level [3].

$$\begin{aligned} \Delta m^2_{21} = (7.65^{+0.23}_{-0.20}) \times 10^{-5}\ \mathrm{eV}^2, \quad |\Delta m^2_{31}| = (2.40^{+0.12}_{-0.11}) \times 10^{-3}\ \mathrm{eV}^2, \\ \sin^2\theta_{12} = 0.304^{+0.022}_{-0.016}, \quad \sin^2\theta_{23} = 0.50^{+0.07}_{-0.06}, \quad \sin^2\theta_{13} = 0.01^{+0.016}_{-0.011}, \end{aligned} \tag{1}$$

where $\Delta m^2_{ij} = m^2_i - m^2_j$, m_i being the mass eigenvalue of a neutrino field for $i = 1, 2, 3$. The various θs given above are the mixing angles in the neutrino sector. Apart from the above data, cosmological observations would give an upper bound on the neutrino mass scale to be of the order of 0.1 eV [4]. Such a low mass among the known particle masses can be explained through models based on seesaw mechanism [5]. A consequence of seesaw mechanism is the existence of neutrinoless double beta decay process [6], which is being investigated in experiments. The mixing angles in eq. (1) suggest that there should be two large and one small angles in the neutrino sector, whose pattern is very much different from that in the quark sector where all the three mixing angles are small. This issue also indicates new physics for which a model has been proposed [7]. Moreover, the central values of the three mixing angles in eq. (1) are very close to the tri-bimaximal pattern which is given below [8]

$$\sin\theta^{\mathrm{TB}}_{12} = \frac{1}{\sqrt{3}}, \quad \sin\theta^{\mathrm{TB}}_{23} = \frac{1}{\sqrt{2}}, \quad \sin\theta^{\mathrm{TB}}_{13} = 0. \tag{2}$$

Several models based on discreet symmetries have been motivated to explain the tri-bimaximal pattern in the neutrino sector [9].

On the other hand, the anomalous magnetic moment of muon is one of the most precisely measured quantities in experiments, which can be quantified as $a_\mu = (g-2)_\mu/2$. After the recent experiment E821 at the Brookhaven National Laboratory, a world average of [10]

$$a^{\mathrm{EXP}}_\mu = 11659208.0(6.3) \times 10^{-10} \tag{3}$$

has been achieved with a precision of 0.54 parts per million. Various groups have computed the theoretical value of a_μ in the standard model (SM), i.e. a^{SM}_μ. The uncertainty in computing the a^{SM}_μ is largely coming from the hadronic loop corrections. For a review on the calculational methods and results of a^{SM}_μ, see [11, 12]. The results from these groups indicate that the experimental value a^{EXP}_μ differs from the theoretically calculated value a^{SM}_μ by about $2-3\ \sigma$. Although some work needs to be done to reduce the size of error bars on the a_μ in the SM, at this moment it is tempting to say that this difference indicates physics beyond the SM. In this work, we have taken the difference between the experiment and the SM value of a_μ as [13]

$$\Delta a_\mu = a^{\mathrm{EXP}}_\mu - a^{\mathrm{SM}}_\mu = (27.7 \pm 9.3) \times 10^{-10}. \tag{4}$$

Supersymmetry [14] is a leading candidate for physics beyond the SM. In some class of supersymmetric models where the lepton number is assumed to be violated, the neutrino masses and mixing angles can be understood. Among these, bilinear R-parity violating

(BRpV) supersymmetric model [15] has rich phenomenology [16] and simple structure to explain the neutrino masses and mixing angles [17–19]. In the BRpV supersymmetric model, a single neutrino acquires non-zero mass at the tree level through a mixing between flavor neutrinos and neutralinos. The remaining two neutrinos acquire masses at 1-loop level, among which the dominant diagrams are generated through the neutralino−sneutrino−Higgs loops. Since neutralinos are playing a part in giving masses to the neutrinos, the parameters of neutralinos obviously determine the neutrino masses in this model. The neutrino masses generated at 1-loop level also depend on some supersymmetry breaking soft parameters due to the presence of sneutrinos and Higgses in the loop. Interestingly, the parameters related to neutralinos and sneutrino masses also determine the $(g-2)_\mu$ in the BRpV supersymmetric model. This is due to the fact that the leading supersymmetric contribution to the $(g-2)_\mu$ in this model comes from 1-loop diagrams generated by neutralino−smuon and chargino−muon-sneutrino loops, where the chargino masses are determined by the parameters of neutralino matrix. Since both the neutrino mass-squares and the $(g-2)_\mu$ have been measured precisely, it is interesting to see if these two set of observable quantities can put constraints on the above said parameters in the BRpV supersymmetric model, which is the aim of this work.

The paper has been organized as follows. In Sec. II we briefly describe the BRpV supersymmetric model and how neutrinos acquire masses at tree and 1-loop levels. We also briefly explain the supersymmetric contribution from the BRpV model to the $(g-2)_\mu$. In Sec. III we describe our method of analyzing constraints on the model parameters due to the neutrino masses and the $(g-2)_\mu$, and also present our results. We conclude in Sec. IV.

II. THE MODEL, NEUTRINO MASSES AND $(g-2)_\mu$

The superpotential of the BRpV supersymmetric model is

$$W = Y_u^{ij}\hat{Q}_i\hat{U}_j\hat{H}_u - Y_d^{ij}\hat{Q}_i\hat{D}_j\hat{H}_d - Y_e^{ij}\hat{L}_i\hat{E}_j\hat{H}_d + \mu\hat{H}_u\hat{H}_d + \epsilon_i\hat{L}_i\hat{H}_u, \tag{5}$$

where the indices i, j run from 1 to 3. The superfields $\hat{Q}$, $\hat{U}$ and $\hat{D}$ are doublet, singlet up-type and singlet down-type quark fields, respectively. $\hat{L}$ and $\hat{E}$ are doublet and singlet charged lepton superfields, respectively. $\hat{H}_u$ and $\hat{H}_d$ are up- and down-type Higgs superfields, respectively. The bilinear term $\hat{H}_u\hat{H}_d$ is called μ-term and the mass parameter μ is assumed to be $\mathcal{O}(100)$ GeV, in order to have theoretical consistency of the model. The other bilinear term $\hat{L}\hat{H}_u$ violates lepton number as well as R-parity and it is called BRpV term. Along with the supersymmetry conserving terms of eq. (5), we also get soft terms in the low energy regime as a result of supersymmetry breaking in the high energy scale. Below we give those soft terms in the scalar potential, which are necessary for both the neutrino masses and the $(g-2)_\mu$.

$$\begin{aligned} V_{\text{soft}} = {} & \frac{1}{2}M_1\tilde{B}\tilde{B} + \frac{1}{2}M_2\tilde{W}\tilde{W} + (m_L^2)_{ij}\tilde{L}_i^*\tilde{L}_j + (m_E^2)_{ij}\tilde{E}_i^*\tilde{E}_j + (A_E Y_E)_{ij}\tilde{L}_i\tilde{E}_j H_d \\ & + (b_\mu)H_u H_d + (b_\epsilon)_i\tilde{L}_i H_u + \cdots, \end{aligned} \tag{6}$$

where the first two terms in the above equation are mass terms for $\mathrm{U}(1)_Y$ and $\mathrm{SU}(2)_L$ gaugino fields, respectively. The third and fourth terms in the above equation are soft scalar mass terms for the left-handed slepton doublet and right-handed slepton singlet fields,

respectively, and the fifth term is called A-term for slepton fields. The last two terms in the above equation arises due to the μ-term and the BRpV term of eq. (5), respectively.

The BRpV term of eq. (5) allows mixing mass terms between the up-type neutral higgsino field ($\tilde{H}_u^0$) and the three left-handed neutrino fields (ν_i). Also, since lepton number is violated by the BRpV term, the scalar components of left-handed neutrino superfields acquire non-zero vacuum expectation values (vevs). To simplify our formulas, we work in a basis where the vevs of sneutrino fields are zero. For $\psi_N = (\tilde{B}, \tilde{W}^3, \tilde{H}_u^0, \tilde{H}_d^0, \nu_1, \nu_2, \nu_3)^T$, at the tree level we get the following mixing masses: $\mathcal{L} = -\frac{1}{2}\psi_N^T M_N \psi_N + \text{h.c.}$, where

$$M_N = \begin{pmatrix} M_{\chi^0} & m \\ m^T & 0 \end{pmatrix}, \tag{7}$$

$$M_{\chi^0} = \begin{pmatrix} M_1 & 0 & \frac{1}{\sqrt{2}} g_1 v_u & -\frac{1}{\sqrt{2}} g_1 v_d \\ 0 & M_2 & -\frac{1}{\sqrt{2}} g_2 v_u & \frac{1}{\sqrt{2}} g_2 v_d \\ \frac{1}{\sqrt{2}} g_1 v_u & -\frac{1}{\sqrt{2}} g_2 v_u & 0 & -\mu \\ -\frac{1}{\sqrt{2}} g_1 v_d & \frac{1}{\sqrt{2}} g_2 v_d & -\mu & 0 \end{pmatrix}, \quad m = \begin{pmatrix} 0 & 0 & 0 \\ 0 & 0 & 0 \\ \epsilon_1 & \epsilon_2 & \epsilon_3 \\ 0 & 0 & 0 \end{pmatrix}. \tag{8}$$

Here, g_1, g_2 are the gauge couplings corresponding to $\text{U}(1)_Y$ and $\text{SU}(2)_L$, respectively. For the vevs of Higgs scalar fields we have followed the convention: $\langle H_d^0 \rangle = v_d = v \cos\beta, \langle H_u^0 \rangle = v_u = v \sin\beta$, where $v = 174$ GeV is the electroweak scale. For $\epsilon_i << m_{\text{susy}} \sim$ TeV, the left-handed neutrinos acquire non-zero masses through a seesaw mechanism at around TeV scale. At the tree level, upto leading order in the expansion of $\frac{1}{m_{\text{susy}}}$, the neutrino masses would be determined by $m_\nu = -m^T M_{\chi^0}^{-1} m$. It can be easily seen that after plugging eq. (8) in this expression, only one neutrino mass eigenvalue would be non-zero. The other two neutrino eigenstates get masses at 1-loop level, for which many different possible loop diagrams exist. However, it has been argued in Ref. [19] that in the case where the tree level neutrino mass eigenvalue is dominant, the 1-loop generated by two insertions of b_ϵ would be the dominant one among all the loop diagrams for the neutrinos, which is the case we consider in this work.

For simplicity, we assume that the sneutrinos are degenerate. In such a case the dominant contribution to the neutrino mass matrix can be written as [18, 19]

$$(m_\nu)_{ij} = a_0 \epsilon_i \epsilon_j + a_1 (b_\epsilon)_i (b_\epsilon)_j, \tag{9}$$

where the indices i, j run from 1 to 3. The first term in the above equation is due to the tree level effect and the second term is from the 1-loop diagram. The expressions for a_0 and a_1 are [18, 19]

$$\begin{aligned} a_0 &= \frac{m_Z^2 m_{\tilde{\gamma}} \cos^2\beta}{\mu(m_Z^2 m_{\tilde{\gamma}} \sin 2\beta - M_1 M_2 \mu)}, \quad m_{\tilde{\gamma}} = \cos^2\theta_W M_1 + \sin^2\theta_W M_2, \\ a_1 &= \sum_{i=1}^{4} \frac{(g_2 (U_0)_{2i} - g_1 (U_0)_{1i})^2}{4\cos^2\beta} (m_{N^0})_i \left(I_4(m_h, m_{\tilde{\nu}}, m_{\tilde{\nu}}, (m_{N^0})_i) \cos^2(\alpha - \beta) \right. \\ &\quad \left. + I_4(m_H, m_{\tilde{\nu}}, m_{\tilde{\nu}}, (m_{N^0})_i) \sin^2(\alpha - \beta) - I_4(m_A, m_{\tilde{\nu}}, m_{\tilde{\nu}}, (m_{N^0})_i) \right), \end{aligned} \tag{10}$$

where m_Z is the Z boson mass, θ_W is the Weinberg angle, and the m_h, m_H and m_A are the light, heavy and pseudo-scalar Higgs boson masses, respectively. The unitary matrix U_0 diagonalizes the neutralino matrix M_{χ^0} of eq. (8) and the $(m_{N^0})_i$ are the neutralino

mass eigenvalues. $m_{\tilde{\nu}}$ is the mass of sneutrino field. The angle α is the mixing angle in the rotation matrix which diagonalizes the light and heavy Higgs boson fields. It is to be noted that the Higgs boson masses depend on the soft parameter b_μ which is given in eq. (6). The function I_4 is given by

$$\begin{aligned} I_4(m_1, m_2, m_3, m_4) &= \frac{1}{m_1^2 - m_2^2}[I_3(m_1, m_3, m_4) - I_3(m_2, m_3, m_4)], \\ I_3(m_1, m_2, m_3) &= \frac{1}{m_1^2 - m_2^2}[I_2(m_1, m_3) - I_2(m_2, m_3)], \\ I_2(m_1, m_2) &= -\frac{1}{16\pi^2}\frac{m_1^2}{m_1^2 - m_2^2}\ln\frac{m_1^2}{m_2^2}. \end{aligned} \tag{11}$$

Many of the mass parameters appearing in the above neutrino mass expression are of order a few 100 GeV, except for ϵ_i and $(b_\epsilon)_i$. Taking all the supersymmetric mass scales to be $\mathcal{O}(100$ GeV) and $\tan\beta \sim \mathcal{O}(10)$, the scales of ϵ and b_ϵ should be $\mathcal{O}(10^{-3})$ GeV and $\mathcal{O}(0.1)$ GeV^2, respectively, in order to get a tiny neutrino mass scale of 0.1 eV. In this order of estimation we have taken into account of the partial cancellation of the Higgs boson contributions in the 1-loop [19]. The smallness of the estimated parameters, ϵ and b_ϵ, can be motivated in a supergravity setup [20] and also through other mechanisms [21].

Now, we explain the supersymmetric contribution to the a_μ in the BRpV supersymmetric model, which we quantify as Δa_μ. The forms of the leading 1-loop diagrams to Δa_μ in the BRpV supersymmetric model are the same as that in the minimal supersymmetric standard model (MSSM). In the MSSM the leading contribution to the Δa_μ comes from the neutralino$-$smuon and chargino$-$muon-sneutrino 1-loop diagrams [22]. The corresponding 1-loop diagrams in the BRpV supersymmetric model are such that in the neutralino$-$smuon diagram we have to replace the summation over neutralinos and smuons by neutralino & neutrino states and smuon & charged Higgs states, respectively. Similar modification should be done in the diagram of chargino$-$muon-sneutrino to get the analogous diagram in the BRpV supersymmetric model. However, mixings between the neutralinos & neutrinos, charginos & charged leptons and sleptons & Higgs scalars are suppressed due to the smallness of the neutrino masses. As a result of this, the additional contribution due to neutrinos, charged leptons and Higgs bosons is suppressed in Δa_μ of the BRpV supersymmetric model, and its value would almost be the same as that in the MSSM.

We neglect the off-diagonal elements in the charged slepton and sneutrino mass matrices of eq. (6), which are highly constrained from experimental data on the flavor changing processes [23]. We further neglect the left-right mixing in the smuons, since it is proportional to the muon mass. After neglecting all these various mixing, below we give the leading analytical formula for Δa_μ in the BRpV supersymmetric model, for which the formula would be same

as that in the MSSM [22].

$$
\begin{aligned}
\Delta a_\mu &= \Delta a_\mu^{N^0\tilde{\mu}} + \Delta a_\mu^{C^\pm\tilde{\nu}_\mu}, \\
\Delta a_\mu^{N^0\tilde{\mu}} &= \frac{m_\mu}{16\pi^2}\sum_{A,j}\left\{\frac{-m_\mu}{6m^2_{\tilde{\mu}A}(1-x_{Aj})^4}(N^L_{Aj}N^L_{Aj}+N^R_{Aj}N^R_{Aj})(1-6x_{Aj}+3x^2_{Aj}+2x^3_{Aj}-6x^2_{Aj}\ln x_{Aj})\right. \\
&\quad \left. -\frac{(m_{N^0})_j}{m^2_{\tilde{\mu}A}(1-x_{Aj})^3}N^L_{Aj}N^R_{Aj}(1-x^2_{Aj}+2x_{Aj}\ln x_{Aj})\right\}, \\
\Delta a_\mu^{C^\pm\tilde{\nu}_\mu} &= \frac{m_\mu}{16\pi^2}\sum_{j}\left\{\frac{m_\mu}{6m^2_{\tilde{\nu}_\mu}(1-x_j)^4}(C^L_jC^L_j+C^R_jC^R_j)(2+3x_j-6x^2_j+x^3_j+6x_j\ln x_j)\right. \\
&\quad \left. -\frac{(m_{C^\pm})_j}{m^2_{\tilde{\nu}_\mu}(1-x_j)^3}C^L_jC^R_j(3-4x_j+x^2_j+2\ln x_j)\right\}, \\
x_{Aj} &= \frac{(m^2_{N^0})_j}{m^2_{\tilde{\mu}A}}, \quad x_j = \frac{(m^2_{C^\pm})_j}{m^2_{\tilde{\nu}_\mu}}, \quad N^L_{Aj} = -y_\mu(U_0)_{4j}(U_{\tilde{\mu}})_{LA} - \sqrt{2}g_1(U_0)_{1j}(U_{\tilde{\mu}})_{RA}, \\
N^R_{Aj} &= -y_\mu(U_0)_{4j}(U_{\tilde{\mu}})_{RA} + \frac{1}{\sqrt{2}}(g_2(U_0)_{2j}+g_1(U_0)_{1j})(U_{\tilde{\mu}})_{LA}, \\
C^L_j &= y_\mu(U_-)_{2j}, \quad C^R_j = -g_2(U_+)_{1j}.
\end{aligned}
\tag{12}
$$

Here, m_μ, y_μ are the mass and Yukawa coupling of muon, respectively. U_0 is a unitary matrix which diagonalizes the neutralino matrix, given in eq. (8), as $(U_0^T M_{\chi^0} U_0)_{ij} = (m_{N^0})_i\delta_{ij}$, where $i,j = 1,\cdots,4$. U_- and U_+ diagonalizes the chargino matrix

$$
M_C = \begin{pmatrix} M_2 & g_2 v_u \\ g_2 v_d & \mu \end{pmatrix} \tag{13}
$$

as $(U_-^T M_C U_+)_{ij} = (m_{C^\pm})_i\delta_{ij}$, where $i,j = 1,2$. Since we have neglected the left-right mixing in smuon masses, we take its diagonalizing matrix $U_{\tilde{\mu}}$ to be 2×2 unit matrix. After neglecting the left-right mixing, the mass eigenvalues of smuons and muon-sneutrino are

$$
\begin{aligned}
m^2_{\tilde{\mu}1} &= m^2_L + m^2_Z\cos 2\beta(\sin^2\theta_W - \frac{1}{2}), \quad m^2_{\tilde{\mu}2} = m^2_R - m^2_Z\cos 2\beta\sin^2\theta_W, \\
m^2_{\tilde{\nu}_\mu} &= m^2_{\tilde{\nu}} = m^2_L + m^2_Z\cos 2\beta\frac{1}{2}.
\end{aligned}
\tag{14}
$$

Here, m_L, m_R are the soft parameters of left- and right-handed smuons, which are one of the diagonal mass parameters of the third and fourth terms of eq. (6).

From eqs. (9) and (10) it is clear that the neutrino mass eigenvalues depend on the following parameters: $M_1, M_2, \mu, \tan\beta, m_L, \epsilon_i, (b_\epsilon)_i, b_\mu$. From the analytical expression of Δa_μ, which is given in the previous paragraph, we can see that the unknown parameters on which it depends on are: $M_1, M_2, \mu, \tan\beta, m_L, m_R$. The common set of parameters on which both the neutrino masses and the Δa_μ depend on are $M_1, M_2, \mu, \tan\beta, m_L$. As it is explained in Sec. I, since the neutrino masses have been measured accurately and the experimental value of a_μ differs from that of the SM value by about 3σ, it is interesting to analyze them in the BRpV supersymmetric model and see what kind of constraints we may get on the above said common set of parameters. Specifically, we have scanned over the parameters of $M_1, M_2, \mu, \tan\beta$ and have obtained the allowed area on these parameters,

which would satisfy the neutrino masses and the Δa_μ constraints for definite values of m_L, m_R and b_μ. In the scanning procedure we have given some range of values for the unknown parameters ϵ_i and $(b_\epsilon)_i$, which determine the neutrino mass scale. In the next section we elaborate on the procedure of our scanning and present the results.

III. ANALYSIS AND RESULTS

To make our analysis simple, we take the mixing angles in the lepton sector exactly to be the tri-bimaximal pattern as given in eq. (2). Then the unitary matrix which would diagonalize the neutrino mass matrix is

$$U_\nu = \begin{pmatrix} \sqrt{\frac{2}{3}} & \frac{1}{\sqrt{3}} & 0 \\ -\frac{1}{\sqrt{6}} & \frac{1}{\sqrt{3}} & \frac{1}{\sqrt{2}} \\ \frac{1}{\sqrt{6}} & -\frac{1}{\sqrt{3}} & \frac{1}{\sqrt{2}} \end{pmatrix}. \tag{15}$$

Given the mass eigenvalues of the three neutrinos to be m_1, m_2, m_3, and in a basis where the charged lepton mass matrix has been diagonalized, we get the following 3×3 matrix in the flavor space

$$m_\nu = U_\nu^* \begin{pmatrix} m_1 & 0 & 0 \\ 0 & m_2 & 0 \\ 0 & 0 & m_3 \end{pmatrix} U_\nu^\dagger. \tag{16}$$

In the BRpV supersymmetric model, we have already obtained a mass matrix for neutrinos in the flavor space which is given in eq. (9). Equating the above equation to that in eq. (9), we obtain six independent equations. Solving them consistently we get the following solution

$$\begin{aligned} &\epsilon_1 = 0, \epsilon_2 = \epsilon_3 = \epsilon, \quad (b_\epsilon)_1 = (b_\epsilon)_2 = -(b_\epsilon)_3 = b_\epsilon, \\ &m_1 = 0, \quad m_2 = 3a_1(b_\epsilon)^2, \quad m_3 = 2a_0\epsilon^2. \end{aligned} \tag{17}$$

The reason for getting m_1 to be zero is that the rank of matrix in eq. (9) is two, which happens due to the assumption of degenerate sneutrinos. The above solution suggests that we can only have hierarchical mass pattern for the neutrinos. Since we stated before that we consider a scenario where tree level eigenvalue is the dominant one, we set the eigenvalue m_3 to the atmospheric scale $\sqrt{|\Delta m^2_{31}|} \approx 0.05$ eV and the m_2 to the solar scale $\sqrt{\Delta m^2_{21}} \approx 0.009$ eV. Previously, we have estimated the scales of ϵ and b_ϵ to get the right amount of neutrino masses. In this work, to fit the atmospheric and solar neutrino mass scales, we have allowed the values of ϵ to be between $9 \times 10^{-4} - 2 \times 10^{-3}$ GeV and the range for b_ϵ to be 100 times the range of ϵ. To put this statement precisely, the neutrino mass condition with tri-bimaximal mixing pattern is satisfied if the supersymmetric point in the parametric space satisfies the following inequalities

$$9 \times 10^{-4}\ \text{GeV} \leq \sqrt{\frac{0.05\ \text{eV}}{2a_0}} \leq 2 \times 10^{-3}\ \text{GeV}, \quad 0.09\ \text{GeV}^2 \leq \sqrt{\frac{0.009\ \text{eV}}{3a_1}} \leq 0.2\ \text{GeV}^2. \tag{18}$$

The supersymmetric point which satisfies the above condition should also satisfy the restriction due to the Δa_μ which is given in eq. (4). We allow a 2σ variation in eq. (4), and

the condition for a supersymmetric point to be consistent with the $(g-2)_\mu$ is to satisfy the following inequality

$$9.1 \times 10^{-10} \leq \Delta a_\mu \leq 46.3 \times 10^{-10}. \tag{19}$$

At the end of previous section we have stated that our motivation is to scan over the parameters $M_1, M_2, \mu, \tan\beta$ which would satisfy both the neutrino masses and the Δa_μ constraints for some fixed values of m_L, m_R, b_μ in the BRpV supersymmetric model. The parameters b_μ and $\tan\beta$ determine the leading contribution to the Higgs boson masses and also the angle α. In this work we have used the tree level contributions for the Higgs related quantities and fixed the parameter $b_\mu = (100\ \text{GeV})^2$. The scanning on the parameters $M_1, M_2, \mu, \tan\beta$ has been done over a grid of points in the following different planes: $M_2 - M_1$, $M_2 - \mu$ and $M_2 - \tan\beta$. Before presenting our results on the scanning, we mention about the lower and upper limiting values for the scanned parameters. From the negative search on supersymmetric particles at the Large Electron Positron collider, we can set a lower limit of 100 GeV on the parameters M_2, μ which determine the chargino masses. From the naturalness argument we can put an upper limit on these to be around 1 TeV. Based on these facts, we take lower and upper limiting values on the mass parameters M_1, M_2, μ to be 100 GeV and 1 TeV, respectively. For $\tan\beta$, we scan over positive values from 1 to 20.

In the scanning on the parameters of neutralinos, we have found that $\tan\beta$ can be constrained severely from the solar neutrino mass scale. Hence we first present our scanning results in the plane $M_2 - \tan\beta$. We consider points of the form $(100+m2\times 20\ \text{GeV}, 1+t\times 0.2)$ in the plane $M_2 - \tan\beta$, where the integers $m2$ and t vary from 0 to 45 and 0 to 95, respectively. Essentially, the above set of points give a rectangular grid in the plane $M_2 - \tan\beta$, with a step size of 20 GeV in the M_2 and 0.2 in the $\tan\beta$ axes, respectively. At each point on this plane we vary M_1 and μ from 100 GeV to 1 TeV in steps of 5 GeV, and verify if the conditions due to neutrino masses, as given in eq. (18), and the condition due to Δa_μ, as given in eq. (19), are satisfied. We have also done the above said scanning by checking the constraints due to either neutrino masses or the Δa_μ, to understand the individual constraints from both these observable quantities.

In Fig. 1(a) we have given allowed set of points in the plane $M_2 - \tan\beta$ for $m_L = 200$ GeV by the neutrino mass constraint of eq. (18). The $\tan\beta$ is restricted to be less than about 7, and also, no points are allowed in the plane for $\tan\beta$ between about 2 and 4. These stringent limits on the $\tan\beta$ are coming from the solar neutrino mass scale rather than from the atmospheric scale. Numerically, we have seen that for any fixed values of M_1, M_2, μ, the quantity a_1, which is defined in eq. (10), increases with $\tan\beta$ in magnitude upto $\tan\beta \sim 3$ and then decreases afterwards. We have found that at $\tan\beta \sim 3$, the sneutrino mass is almost degenerate with the heavy Higgs and the pseudo-scalar Higgs masses, and hence, the quantity a_1 would be enhanced due to singularity in the function I_4 of eq. (11). For $\tan\beta$ between about 2 to 4 the magnitude of a_1 is so high that the second inequality of eq. (18) is not satisfied. After reaching the maximum at $\tan\beta \sim 3$, the quantity a_1 would decrease in magnitude with increasing $\tan\beta$, due to increase in the masses of heavy and pseudo-scalar Higgses. So, for $\tan\beta$ greater than 7, the magnitude of a_1 would come out to be so less that the second inequality in eq. (18) is not satisfied.

For $m_L = 200$ GeV and $m_R = 300$ GeV, we have given the allowed points in the plane $M_2 - \tan\beta$ due to the Δa_μ constraint of eq. (19) in Fig. 1(b). From the figure it can be noticed that by increasing the M_2 values the lower limit on $\tan\beta$ is increasing. This fact can be understood from the dependences of Δa_μ on relevant parameters. Numerically, we have seen that the Δa_μ is inversely proportional to either M_2 or μ and it is directly proportional

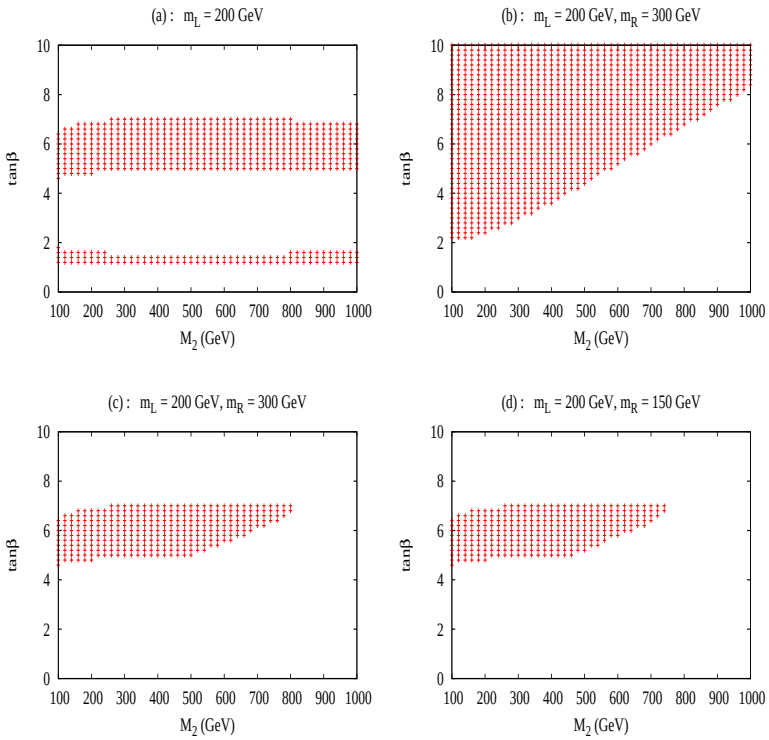

FIG. 1. Allowed space in the plane $M_2 - \tan\beta$. In the upper-left and upper-right plots, only the neutrino mass and Δa_μ constraints have been applied, respectively. In the lower-left and lower-right plots, both the neutrino mass and Δa_μ constraints have been applied for different set of soft parameters m_L, m_R. For details, see the text.

to $\tan\beta$ [24]. For $m_R > m_L$, which is the case in Fig. 1(b), the dependence of M_1 on Δa_μ is negligible, since the $\Delta a_\mu^{C^\pm \tilde{\nu}_\mu}$ of eq. (12) would dominate over the $\Delta a_\mu^{N^0 \tilde{\mu}}$. Now, it is easy to understand that by increasing M_2 the value of Δa_μ may come below the lower limit of eq. (19), which can be compensated by increasing $\tan\beta$, and thus we get the allowed space as shown in Fig. 1(b).

In Fig. 1(c) we have given allowed points by both the eqs. (18) and (19) in the plane $M_2 - \tan\beta$ for $m_L = 200$ GeV and $m_R = 300$ GeV. Essentially, the points in Fig. 1(c) are almost the intersection of the points of Figs. 1(a) and 1(b). By combining the neutrino mass constraints with the constraint due to the Δa_μ, we can get upper bound on the M_2 which is shown in Fig. 1(c). In Fig. 1(d) we have given allowed points by both the eqs. (18) and (19) in the plane $M_2 - \tan\beta$ for $m_L = 200$ GeV and $m_R = 150$ GeV. The value of m_R in Fig. 1(d) is less than that in Fig. 1(c). The parameter m_R affect the $\Delta a_\mu^{N^0 \tilde{\mu}}$ of eq. (12). Numerically, we have seen that the quantity $\Delta a_\mu^{N^0 \tilde{\mu}}$ would give negative contribution and its magnitude is less than that of $\Delta a_\mu^{C^\pm \tilde{\nu}_\mu}$ which gives positive values. By decreasing the value of m_R the negative contribution due to neutralinos would increase in magnitude, and as a result the net Δa_μ decreases from its previous value. Since the Δa_μ also decreases with increasing the M_2, we loose some more points on the higher end of M_2, which can be seen by comparing Fig. 1(d) with Fig. 1(c).

In the plots of Fig. 1, the values of m_L and m_R are somewhat low. By increasing these values we have done a similar scanning in the plane $M_2 - \tan\beta$ to illustrate how the

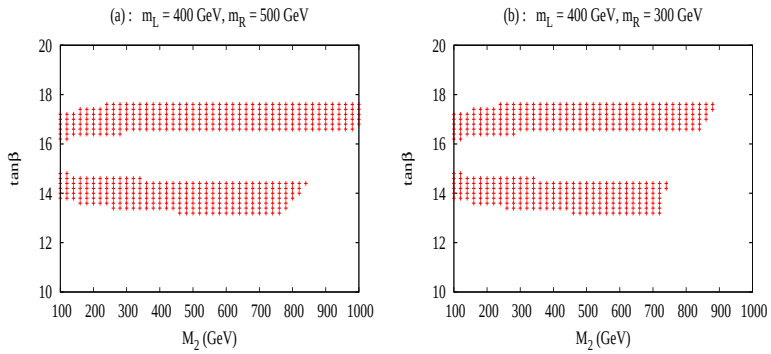

FIG. 2. Allowed space in the plane $M_2 - \tan\beta$ by both the neutrino mass and the Δa_μ constraints. The values of m_L, m_R are higher in this case as compared to that in Fig. 1.

constraints would change quantitatively. In Figs. 2(a) and 2(b) we have applied constraints due to eqs. (18) and (19), for $(m_L, m_R) = (400\text{ GeV}, 500\text{ GeV})$ and $(400\text{ GeV}, 300\text{ GeV})$, respectively. The allowed $\tan\beta$ in these plots is between about 13 and 18, whose values are high compared to that in Fig. 1. For $\tan\beta$ either larger than 18 or lesser than 13 the quantity a_1 is suppressed, and for $\tan\beta$ between about 15 and 16 the a_1 is enhanced, so that the second inequality of eq. (18) is not satisfied. The reasons for suppression or enhancement of a_1 in this case is analogous to the case of Fig. 1(a). On top of these neutrino mass constraints, the constraint due to Δa_μ can eliminate points on the higher end of M_2, which is evident in Fig. 2(a). The effect of negative enhanced contribution of the neutralino diagram to Δa_μ, which we explained in the previous paragraph, can be seen in Fig. 2(b).

We now give the results of scanning in the plane $M_2 - \mu$. In order to have a grid of points in this plane, we consider points of the form $(100 + m2 \times 20\text{ GeV}, 100 + m \times 20\text{ GeV})$, where the integers $m2, m$ vary independent of one another from 0 to 45. Basically, these set of points form a grid in the plane $M_2 - \mu$ with a step size of 20 GeV in both the M_2 and μ axes. Since we have known the allowed $\tan\beta$ from Figs. 1 and 2, at each point on the grid of the plane $M_2 - \mu$, we run M_1 from 100 GeV to 1 TeV in steps of 5 GeV and vary $\tan\beta$ either from 1 to 7 in steps of 0.2 if m_L is 200 GeV or from 13 to 18 in steps of 0.2 if m_L is 400 GeV.

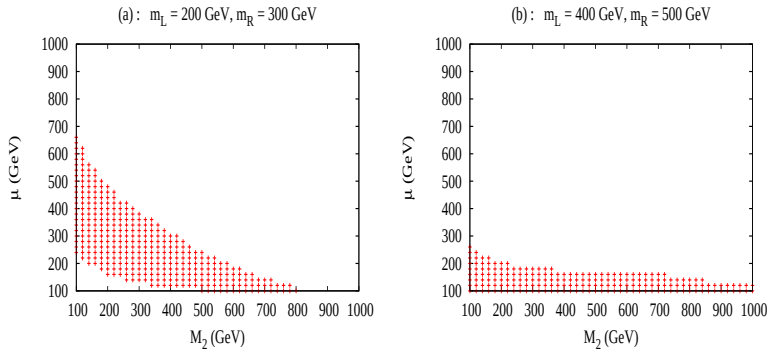

FIG. 3. Allowed space in the plane $M_2 - \mu$ by both the neutrino mass and the Δa_μ constraints for two different set of (m_L, m_R) values.

In Fig. 3(a) we have given allowed points by both the neutrino mass and the Δa_μ constraints for $(m_L, m_R) = (200\text{ GeV}, 300\text{ GeV})$. In this plot, the white area in the lower-

left corner where both M_2 and μ are small is disallowed because the tree level neutrino mass eigenvalue cannot fit the atmospheric scale. The atmospheric scale is determined by the quantity a_0 which decreases with increasing either μ or $\tan\beta$, which can be seen from eq. (10). Since the solar scale demands that the $\tan\beta$ to be less than about 7 for $m_L = 200$ GeV, the quantity a_0 would be so high for low values of μ, M_2. These high values of a_0 do not satisfy the first inequality of eq. (18). The vast white area on the top-right side of the allowed narrow strip is disallowed because the values of Δa_μ are coming out to be smaller than the lower limit of eq. (19), which can be understood from the dependences of Δa_μ on the relevant parameters.

In Fig. 3(a) m_L is fixed to 200 GeV. The results of scanning over the plane $M_2 - \mu$ can dramatically change if we increase m_L to 400 GeV. In Fig. 3(b) we have given the allowed points by both the neutrino mass and the Δa_μ constraints for $(m_L, m_R) = (400$ GeV, 500 GeV). In this plot, the μ is constrained to be within 260 GeV. The allowed $\tan\beta$ range in this case is somewhat large and gives suppression in the quantity a_0 of eq. (10). The a_0 further gets suppression if μ is larger than 260 GeV so that the first inequality of eq. (18) is not satisfied. Unlike in Fig. 3(a), the role of Δa_μ constraint is very minimal and the majority of constraints in Fig. 3(b) are due to neutrino masses. In both the plots of Fig. 3 the parameter m_L is less than that of m_R. By setting $m_L > m_R$, we may see a reduction in the number of points in the higher end of M_2, due to negative enhanced neutralino contribution of Δa_μ.

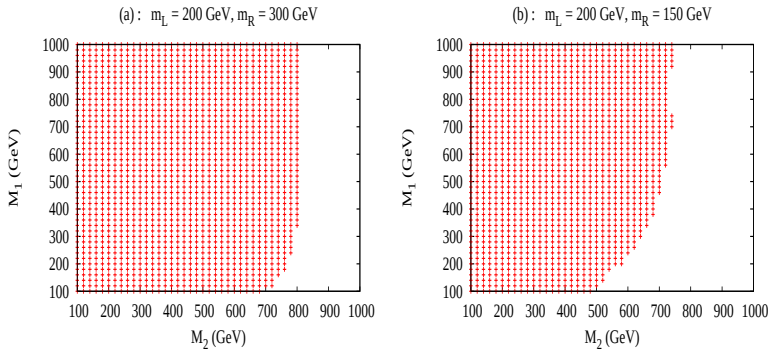

FIG. 4. Allowed space in the plane $M_2 - M_1$ by both the neutrino mass and the Δa_μ constraints for two different sets of (m_L, m_R) values.

Our method of doing scanning in the plane $M_2 - M_1$ is similar to what we have done in the plane $M_2 - \mu$. If we replace μ with M_1 and vice versa in the scanning of $M_2 - \mu$, which we have described previously, this would give scanning in the plane $M_2 - M_1$. In Figs. 4(a) & 4(b) we have given allowed parametric space in this plane due to neutrino masses and the Δa_μ constraints for $(m_L, m_R) = (200$ GeV, 300 GeV) and (200 GeV, 150 GeV), respectively. The exclusion area in these plots, which is shown in white area, can be understood from the properties of the neutrino masses and the Δa_μ, which we have described previously. Although there is some exclusion area in Figs. 4(a) & 4(b), there is no upper bound on the M_1 parameter unlike an upper bound on the M_2, which can be seen in the above plots. This implies that the parameter M_1 is not sensitive to either of the neutrino mass eigenvalues and to the Δa_μ as well. We have repeated the above scanning in the plane $M_2 - M_1$ by increasing the (m_L, m_R) values. Even in this case we have found that there could be some exclusion area in the above plane but no stringent bounds on the parameter M_1.

One comment on our scanning results is that we have fixed the soft parameter of the bilinear Higgs term b_μ to be $(100\ \text{GeV})^2$, which determines the Higgs boson masses at tree level. By changing this parametric value, the white disallowed area in Figs. 1 and 2 which happens due to the degeneracy of the sneutrino mass and the Higgs boson masses, may change quantitatively. For a related work on the consistency of neutrino masses and $(g-2)_\mu$, see [25].

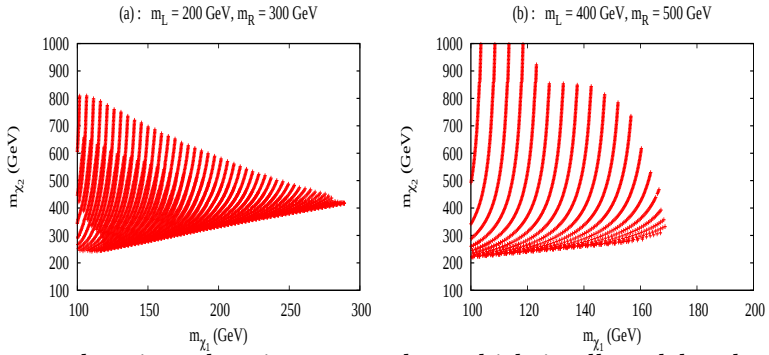

FIG. 5. Lightest versus heaviest chargino mass plot, which is allowed by the constraints due to neutrino masses and the Δa_μ. $m_{\chi 1}$ and $m_{\chi 2}$ are the lightest and the heaviest chargino masses, respectively. For details, see the text.

Finally, we give one of the applications of our scanning procedure. One of the main channels to probe supersymmetry in experiments is the production of chargino and its decay to lighter particles. In this context it would be interesting if we can find some upper bounds on the chargino masses in the present model. The tree level chargino masses are determined by the following parameters: M_2, μ and $\tan\beta$. In Figs. 3(a) & 3(b), we have given the allowed parametric space in the plane $M_2 - \mu$ due to both the neutrino masses and the Δa_μ constraints. Since we know the $\tan\beta$ range in both these plots, we can calculate the lowest and the heaviest chargino masses at each allowed point of the plane $M_2 - \mu$. To get the results for chargino masses we take the grid step size to be 5 GeV in the M_2 and μ axes. At each point on this grid we vary M_1 and $\tan\beta$ as it has been done in Figs. 3(a) & 3(b). We also fix the necessary soft parameters to the values as they are taken in Figs. 3(a) & 3(b). In Fig. 5 we have given the plots for the lightest (m_{χ_1}) versus heaviest (m_{χ_2}) chargino masses which are allowed by the neutrino masses and the Δa_μ constraints. The empty space between some contour kind of lines in these plots is happening due to finite grid step size of the plane $M_2 - \mu$. From these plots we can see that for a definite value of lightest chargino mass we can get an upper and lower bounds on the heaviest chargino mass, and vice versa. In Fig. 5(a) for $m_{\chi_1} = 150$ GeV, the lower and upper bounds on the heaviest chargino mass are 270 GeV and 700 GeV, respectively. Whereas, in Fig. 5(b) for the same $m_{\chi_1} = 150$ GeV, the value of m_{χ_2} lies between about 250 GeV and 800 GeV. Also, depending on the values of the soft masses we can get an absolute upper bound on the lightest chargino mass. In Fig. 5(a), the absolute upper bound on the lightest chargino is about 290 GeV, whereas, in Fig. 5(b) it is about 170 GeV.

IV. CONCLUSIONS

The smallness of neutrino masses and the 3σ deviation of the experimental value of the muon $(g-2)_\mu$ from that of the standard model value, may indicate new physics. We have

studied how the observed values of these two quantities put constraints on some parametric values in the bilinear R-parity violating supersymmetric model. One interesting feature of this model is that the parameters which determine the neutralino and chargino masses also determine the neutrino masses as well as the Δa_μ. The neutrino masses and the Δa_μ depend on some soft parameters as well. By taking these soft parameters to some fixed values, we have scanned over the following parameters: M_1, M_2, μ and $\tan\beta$, and presented allowed parametric space by satisfying the observed data on the neutrino masses and the Δa_μ. For neutrino mixing angles, we have assumed the tri-bimaximal mixing pattern.

The plots we have presented on the allowed parametric space of the parameters, M_1, M_2, μ and $\tan\beta$, are for some specific values of the soft parameters and also for some allowed range of the bilinear parameters ϵ and b_ϵ. In this sense the plots we have given here are only indicative. But, we have described some generic features of the neutrino masses and the Δa_μ and how they play a part in setting bounds on the model parameters. Specifically, we have found that in the BRpV supersymmetric model, depending on the soft parametric values, the constraints due to neutrino masses and the Δa_μ can put certain limits on the parameters $M_2, \mu, \tan\beta$, but not on the parameter M_1. One of the uses of our scanning procedure is that the allowed parametric space we get on the M_2, μ and $\tan\beta$, can set upper and lower bounds on the chargino masses of this model. Indeed, given the data from collider experiments, the results of this scanning procedure can be used to probe the supersymmetric particle spectrum of this model.

ACKNOWLEDGMENTS

The author wishes to thank Xerxes Tata for having some discussions in the initial stages of this work. The author is grateful to Sourov Roy for valuable discussions and suggestions on this work and also for reading the manuscript.

---

[1] R. Davis, Phys. Rev. Lett. **12** 303 (1964); R. Davis *et al.*, Phys. Rev. Lett. **20** 1205 (1968); Y. Fukuda *et. al.* (Kamiokande Collaboration), Phys. Rev. Lett. **77**, 1683 (1996); W. Hampel *et. al.* (Gallex Collaboration), Phys. Lett. B **447**, 127 (1999); J.N. Abdurashitov *et. al.* (SAGE Collaboration), Phys. Rev. C **60**, 055801 (1999); Q.R. Ahmad *et. al.* (SNO Collaboration), Phys. Rev. Lett. **87**, 071301 (2001); K. Eguchi *et. al.* (KamLAND Collaboration), Phys. Rev. Lett. **90**, 021802 (2003); J. Hosaka *et. al.* (Super-Kamkiokande Collaboration), Phys. Rev. D **73**, 112001 (2006).

[2] Y. Fukuda *et. al.* (Super-Kamkiokande Collaboration), Phys. Rev. Lett. **81**, 1562 (1998); M. Ambrosio *et. al.* (MACRO Collaboration), Phys. Lett. B **434**, 451 (1998).

[3] T. Schwetz, M.A. Tortola and J.W.F. Valle, New. J. Phys., **10**, 113011 (2008).

[4] S. Hannestad, Nucl. Phys. Proc. Suppl. **145**, 313 (2005); E. Komatsu *et. al.* (WMAP Collaboration), Astrophys. J. Suppl. **180**, 330 (2009).

[5] P. Minkowski, Phys. Lett. B **67**, 421 (1977); T. Yanagida, in *Proceedings of the workshop on unified theory and baryon number in the universe*, KEK, March 1979, eds. O. Sawada and A. Sugamoto; M. Gell-Mann, P. Ramond and R. Slansky, in *Supergravity*, Stonybrook, 1979, eds. D. Freedman and P. van Nieuwenhuizen; S.L. Glashow, *The future of elementary particle physics*, in *Proceedings of the 1979 Cargèse Summer Institute on Quarks and Leptons* (M. Lévy

et al. eds.), Plenum Press, New York, 1980, pp. 687; R.N. Mohapatra and G. Senjanović, Phys. Rev. Lett. **44**, 912 (1980); J. Schechter and J.W.F. Valle, Phys. Rev. D **22**, 2227 (1980); G.B. Gelmini and M. Roncadelli, Phys. Lett. B **99**, 411 (1981).

[6] H.V. Klapdor-Kleingrothaus, I.V. Krivosheina, A. Dietz and O. Chkvorets, Phys. Lett. B **586**, 198 (2004).

[7] Y. Achiman, J. Erler and W. Kalau, Nucl. Phys. B **331**, 213 (1990).

[8] P.F. Harrison, D.H. Perkins and W.G. Scott, Phys. Lett. B **530**, 167 (2002).

[9] E. Ma and G. Rajasekaran, Phys. Rev. D **64**, 113012 (2001); J. Kubo, A. Mondragon, M. Mondragon and E. Rodriguez-Jauregui, Prog. Theor. Phys. **109**, 795 (2003); E. Ma, Phys. Rev. D **70**, 031901(R) (2004); New. J. Phys. **6**, 104 (2004); G. Altarelli and F. Feruglio, Nucl. Phys. B **720**, 64 (2005).

[10] G.W. Bennet *et. al.* (Muon G-2 Collaboration), Phys. Rev. D **73**, 072003 (2006).

[11] Z. Zhang, arXiv:0801.4905 [hep-ph]; F. Jegerlehner and A. Nyffeler, Phys. Rept., **477**, 1 (2009).

[12] T. Teubner, K. Hagiwara, R. Liao, A.D. Martin and D. Nomura, arXiv:1001.5401 [hep-ph]; C.S. Fischer, T. Goecke and R. Williams, arXiv:1009.5297 [hep-ph]; M. Davier, A. Hoecker, B. Malaescu and Z. Zhang, arXiv:1010.4180 [hep-ph]; T. Goecke, C.S. Fischer, T. Goecke and R. Williams, arXiv:1012.3886 [hep-ph].

[13] F. Domingo and U. Ellwanger, JHEP, 0807, 079 (2008).

[14] H.P. Nilles, Phys. Rept. **110**, 1 (1984); H.E. Haber and G.L. Kane, Phys. Rept. **117**, 75 (1985); S.P. Martin, arXiv:hep-ph/9709356; M. Drees, R. Godbole and P. Roy, Theory and Phenomenology of Sparticles, (World Scientific, 2004); P. Binetruy, Supersymmetry (Oxford University Press, 2006); H. Baer and X. Tata, Weak Scale Supersymmetry: From Superfields to Scattering Events, (Cambridge University Press, 2006).

[15] M. Hirsch and J.W.F. Valle, New J. Phys. **6**, 76 (2004).

[16] S. Roy and B. Mukhopadhyaya, Phys. Rev. D **55**, 7020 (1997); B. Mukhopadhyaya, S. Roy and F. Vissani, Phys. Lett. B **443**, 191 (1998); S.Y. Choi, E.J. Chun, S.K. Kang and J.S. Lee, Phys. Rev. D **60**, 075002 (1999); W. Porod, M. Hirsch, J. Romao and J.W.F. Valle, Phys. Rev. D **63**, 115004 (2001); M. Hirsch, W. Porod, J.C. Romao and J.W.F. Valle, Phys. Rev. D **66**, 095006 (2002); A. Bartl, M. Hirsch, T. Kernreiter, W. Porod and J.W.F. Valle, JHEP, 0311, 005 (2003); F. de Campos, O.J.P. Eboli, M.B. Magro, W. Porod, D. Restrepo, M. Hirsch and J.W.F. Valle, JHEP, 0805, 048 (2008).

[17] M. Hirsch, M.A. Diaz, W. Porod, J.C. Romao and J.W.F. Valle, Phys. Rev. D **62**, 113008 (2000); M.A. Diaz, M. Hirsch, W. Porod, J.C. Romao and J.W.F. Valle, Phys. Rev. D **68**, 013009 (2003).

[18] S. Davidson and M. Losada, JHEP, 0005, 021 (2000); Phys. Rev. D **65**, 075025 (2002).

[19] Y. Grossman and S. Rakshit, Phys. Rev. D **69**, 093002 (2004).

[20] R.S. Hundi, S. Pakvasa and X. Tata, Phys. Rev. D **79**, 095011 (2009).

[21] A. Masiero and J.W.F. Valle, Phys. Lett. B **251**, 273 (1990); J.C. Romao, C.A. Santos and J.W.F. Valle, Phys. Lett. B **288**, 311 (1992); J.C. Romao, A. Ioannisian and J.W.F. Valle, Phys. Rev. D **55**, 427 (1997).

[22] P. Fayet, in *Unification of the Fundamental Particles Interactions*, eds. S. Ferrara, J. Ellis, P. van Nieuwenhuizen, (Plenum, NY, 1980); J.A. Grifols and A. Mendez, Phys. Rev. D **26**, 1809 (1982); J.R. Ellis, J.S. Hagelin and D.V. Nanopoulos, Phys. Lett. B **116**, 283 (1982); R. Barbieri and L. Maiani, Phys. Lett. B **117**, 203 (1982); D.A. Kosower, L.M. Krauss and N. Sakai, Phys. Lett. B **133**, 305 (1983); T.C. Yuan, R.L. Arnowitt, A.H. Chamseddine and

P. Nath, Z. Phys. C **26**, 407 (1984); J.C. Romao, A. Barroso, M.C. Bento and G.C. Branco, Nucl. Phys. B **250**, 295 (1985); I. Vendramin, Nuovo Cim. A **101**, 731 (1989); S.A. Abel, W.N. Cottingham and I.B. Whittingham, Phys. Lett. B **259**, 307 (1991); J.L. Lopez, D.V. Nanopoulos and X. Wang, Phys. Rev. D **49**, 366 (1994); U. Chattopadhyay and P. Nath, Phys. Rev. D **53**, 1648 (1996); T. Moroi, Phys. Rev. D **53**, 6565 (1996) [Erratum-ibid. D **56**, 4424 (1997)]; S.P. Martin and J.D. Wells, Phys. Rev. D **64**, 035003 (2001).

[23] M.L. Brooks *et. al.* (MEGA Collaboration), Phys. Rev. Lett. **83**, 1521 (1999); M. Ahmed *et. al.* (MEGA Collaboration), Phys. Rev. D **65**, 112002 (2002).

[24] See, the last four articles of Ref. [22].

[25] T. Fukuyama, T. Kikuchi and N. Okada, Phys. Rev. D **68**, 033012 (2003).